

Fermi-surface-induced lattice modulation and charge-density wave in optimally doped $\text{YBa}_2\text{Cu}_3\text{O}_{7-x}$

X. Liu,¹ Z. Islam,² S. K. Sinha,¹ S. C. Moss,³ R. J. McQueeney,⁴ J. C. Lang,² and U. Welp⁵

¹Department of Physics, University of California, San Diego, 9500 Gilman Drive, La Jolla, California 92093, USA

²Advanced Photon Source, Argonne National Laboratory, 9700 S. Cass Avenue, Argonne, Illinois 60439, USA

³Department of Physics and Texas Center for Superconductivity, University of Houston, Houston, Texas 77204, USA

⁴Department of Physics and Astronomy, Iowa State University, Ames, Iowa 50011, USA

⁵Materials Science Division, Argonne National Laboratory, Argonne, Illinois 60439, USA

(Received 25 August 2008; revised manuscript received 23 September 2008; published 28 October 2008)

We have observed a Fermi-surface (FS) induced lattice modulation in a $\text{YBa}_2\text{Cu}_3\text{O}_{7-x}$ superconductor with a wave vector along CuO chains; i.e., $\mathbf{q}_1 = (0, \delta, 0)$. The value of $\delta \sim 0.21$ is twice the Fermi wave vector ($2\mathbf{k}_F$) along \mathbf{b}^* connecting nearly nested FS “ridges.” The \mathbf{q}_1 modulation exists only within O-vacancy-ordered islands [characterized by $\mathbf{q}_0 = (\frac{1}{4}, 0, 0)$] and persists well above and below T_c . Our results are consistent with the presence of a FS-induced charge-density wave.

DOI: 10.1103/PhysRevB.78.134526

PACS number(s): 74.25.Jb, 61.05.cp, 71.45.Lr, 74.72.Bk

I. INTRODUCTION

The optimal doped cuprate superconductor $\text{YBa}_2\text{Cu}_3\text{O}_{7-x}$ (YBCO) is distinguished by the presence of CuO chains which are parallel to the orthorhombic \mathbf{b} axis and interleaved with CuO_2 bilayers approximately 0.4 nm away. This compound provides the opportunity for the CuO₂ planes to interact with a subsystem of different dimension and symmetry. This uniqueness has attracted a lot of attention, both experimentally¹⁻⁴ and theoretically.⁵⁻⁹ The chains are believed to be involved in the superconductivity by having a significant portion of the superfluid density associated with them through proximity effect.^{1,4,10} They are also involved in the electronic structure of this compound by contributing flat, nested portions of the Fermi surface perpendicular to the \mathbf{b}^* direction with an incommensurate nesting wave vector $\mathbf{q}_{1C} = (0, 2k_F \approx 0.22, 0)$ (in reduced lattice units; \mathbf{k}_F is the Fermi wave vector) (Fig. 1), as shown by electronic structure calculations¹¹ and confirmed by positron annihilation¹² and photoemission¹³ studies. Such Fermi-surface nesting features are known to give rise to a tendency to an instability against charge-density waves (CDWs) with the periodicity of \mathbf{q}_{1C} and this has led to a number of reports of the existence of such a modulation along the chains.

Evidence for the formation of CDW on the CuO chains has come mainly from surface sensitive scanning tunneling

microscopy (STM) measurements.¹⁴⁻¹⁶ In these measurements, static electronic modulations were observed along the CuO chains with periodicity consistent with the expected \mathbf{q}_{1C} for an optimally doped YBCO. These modulations exhibited short-range correlations and their amplitude appeared to be strongest near the clusters of the chain oxygen vacancies. These authors surmised that the observed electronic modulations could result from dynamic CDW pinned by the vacancy clusters. If the STM observed modulations were a general property of the bulk YBCO, the coexistence of the CDW and superconductivity in the chain subsystem would have a significant effect on the superconducting order parameter and complicate our understanding of superconductivity in YBCO. To our knowledge, there has been no conclusive evidence of the formation of CDW on the chains from bulk-sensitive measurements so far. Local probes such as nuclear magnetic resonance (NMR)/nuclear quadrupole resonance (NQR) measurements¹⁷⁻¹⁹ have reported on the formation of CDW on the CuO chains, but the results of different groups are not consistent with each other. Inelastic neutron scattering (INS) measurements²⁰ have indicated the existence of *dynamical* lattice fluctuations with a wave vector of $(0, \sim 0.23, 0)$, possessing *long-range* coherence. These observations are inconsistent with the STM results. Furthermore, the INS measurements were carried out on a twinned crystal so

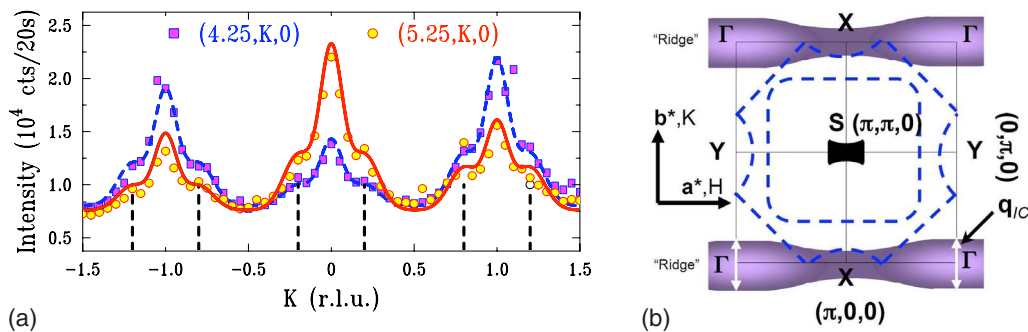


FIG. 1. (Color online) Left: \mathbf{K} scans ($T \sim 7$ K) showing \mathbf{q}_1 shoulders on both sides of the central \mathbf{q}_0 satellite peaks (lines are from Gaussian profile as a guide to the eyes). Vertical dashes indicate the shoulders displaced along \mathbf{K} by ± 0.21 from their respective \mathbf{q}_0 satellite. Right: the schematic of near nesting of the “ridges” (purple) with nesting vector along \mathbf{b}^* (white) (Refs. 12 and 13).

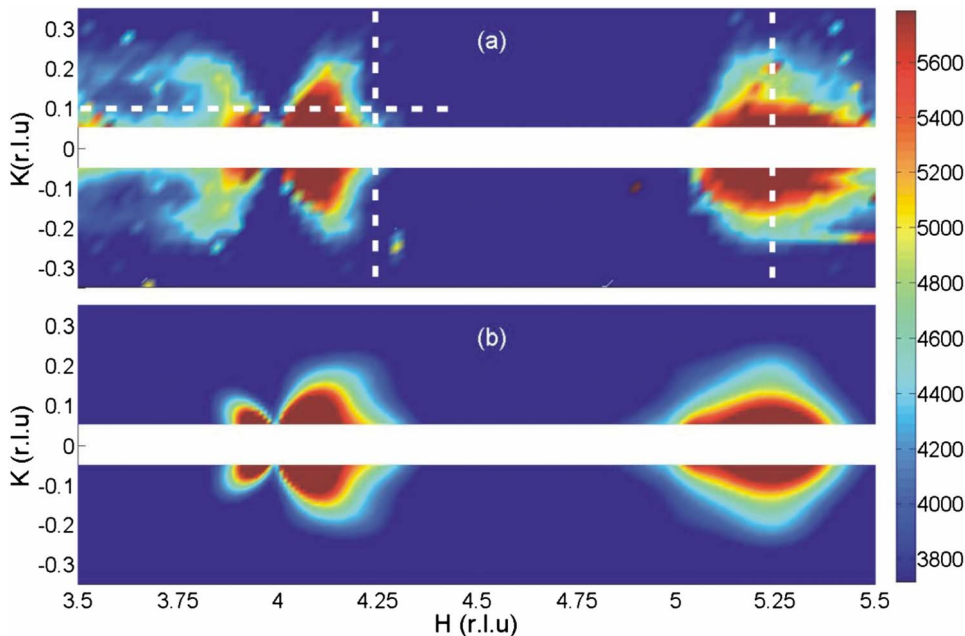


FIG. 2. (Color online) (a) Color map of the measured diffuse scattering around $(4, 0, 0)$ and $(5, 0, 0)$ in H-K plane at ~ 7 K. (b) Model calculations of the two-dimensional (2D) scattering pattern. Asymmetric HDS around $(4, 0, 0)$, \mathbf{q}_0 satellite, and \mathbf{q}_1 shoulders are all reproduced. The dashed lines indicate the line cuts presented in Fig. 3.

that ordering along the \mathbf{a}^* or \mathbf{b}^* axes could not be distinguished.

To further explore the existence of CDW on the CuO chains as a bulk property, we have carried out diffuse x-ray scattering measurements on a high-quality *detwinned* crystal of optimally doped YBCO_{7-x} ($x=0.08$, $T_c=91.5$ K). We show that there are indeed signals corresponding to short-range lattice modulations at the nesting wave vector along the CuO-chain direction (Fig. 1). However, they do not form homogeneously throughout the crystal. Rather, they are confined within the O-ordered ortho-IV phase islands^{21,22} characterized by $\mathbf{q}_0=(\pm\frac{1}{4}, 0, 0)$ (Fig. 1) and give rise to the shoulder structures at \mathbf{q}_1 on both sides of the ortho-IV phase superstructure peaks along \mathbf{b}^* direction as shown in Fig. 1. Our quantitative analysis shows that the atomic displacements of the \mathbf{b} -direction modulations are transverse and primarily along the \mathbf{a} axis. Below we summarize our previous findings then show the coupled nature of the \mathbf{b} -direction modulations and the ortho-IV phase superstructure. A quantitative modeling of the diffuse-scattering pattern (Fig. 2) is used to establish the source of the \mathbf{q}_1 shoulders.

II. RESULTS

High energy ($E=36$ keV) x-ray diffuse-scattering experiments were performed on the X-Ray Operations and Research 4-ID-D beam line at the Advanced Photon Source (APS). The choice of high x-ray energy makes this a truly *bulk-sensitive* study.²¹ At this composition, first-principles band calculations²² have shown that the oxygen vacancies, located in the chains, tend to cluster together to form a minority phase with a four-unit-cell superstructure, corresponding to a sequence of three O-full and one O-vacant chains (ortho-IV phase denoted by $\langle 1110 \rangle$, see Fig. 4), respectively, the formation of which was confirmed in a previous x-ray scattering study.²¹ That study revealed that, in the ortho-IV phase islands, coupled displacements of Ba, Cu, and O at-

oms, including those in the CuO₂ planes, are induced normal to the \mathbf{b} axis, producing broad satellite peaks centered at $\mathbf{q}_0=(\pm\frac{1}{4}, 0, 0)$ on both sides of Bragg points. Embedded in the average orthorhombic crystal, the ortho-IV phase islands induce long-range strain in the lattice which gives rise to the Huang diffuse scattering (HDS) (Ref. 23) around Bragg peaks [Fig. 2(a)].

If lattice modulations associated with CDWs with propagating vector \mathbf{q}_{IC} are present throughout the whole crystal, they should be observed by x-ray scattering as peaks (or rods) centered at $(m, n, L) \pm \mathbf{q}_{IC}$ (m and n are integers) in the reciprocal space, depending on their interchain correlations. A thorough investigation in the vicinity of $(m, n, L) \pm \mathbf{q}_{IC}$ for different integer m and n values showed no indication of such modulations along \mathbf{b}^* direction as claimed by the INS measurements.²⁰ Instead, clear shoulders were observed at $\mathbf{q}_0 \pm \mathbf{q}_1$, $\mathbf{q}_1=(0, \delta, 0)$ with $\delta \sim 0.2$, as shown in Fig. 1. It is interesting to notice that \mathbf{K} scans through different \mathbf{q}_0 peaks show a definite correlation between the intensities of the shoulder peaks with the center ortho-IV peaks, both having the same correlation lengths and obeying the same parity relations.²¹ The parity relations impose stringent phase correlations between atomic displacements such as those in the ortho-IV model.²¹

Furthermore, careful measurements of the ratio between the satellite and the shoulder intensities as a function of increasing temperature found it to be constant in the range of 7–300 K. As pointed out in Ref. 21, the temperature dependence of the \mathbf{q}_0 peaks distinguishes the ortho-IV phase islands from the average lattice which has less rapidly varying Debye-Waller factors. The fact that the intensities of the shoulders obey the same temperature dependence as the center \mathbf{q}_0 peak strongly indicates that they are intimately related. Therefore, the \mathbf{q}_1 modulation must coexist with ortho-IV islands and does not form homogeneously throughout the crystal.

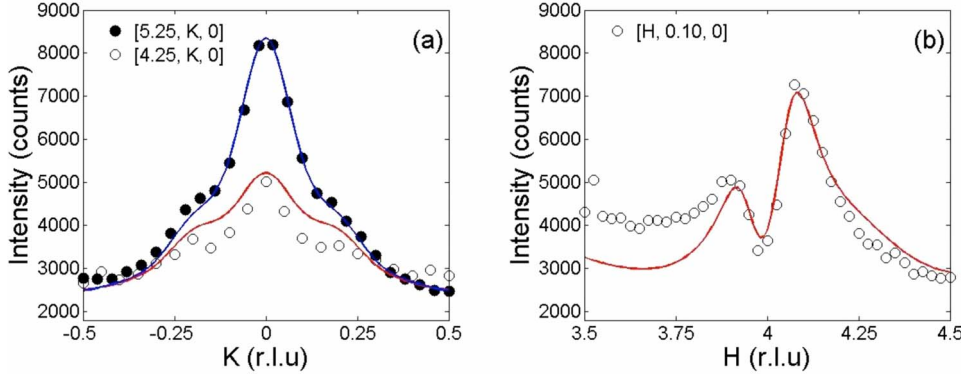


FIG. 3. (Color online) Solid lines are the fitting results. δ and d are determined to be 0.21 and 0.9, respectively. The \mathbf{K} scan in (a) across (4.25, 0, 0) is over estimated by $\sim 13\%$ mainly due to the IFS contribution. The lower side of the \mathbf{H} scan in (b) is pushed up by the tail of strong (3.25, 0, 0) satellite peak.

In order to identify the origin of the shoulders as shown in Fig. 1, two-dimensional scans around several Bragg peaks were performed and the diffuse-scattering intensity pattern around (4, 0, 0) and (5, 0, 0) is shown in Fig. 2(a). The salient feature of this pattern is the profound difference in the symmetry of scattering around the two Bragg peaks. While the dominating feature around the (4, 0, 0) Bragg peak is a strong nearly fourfold “bow-tie”-shape HDS pattern albeit asymmetric, it is entirely missing around (5, 0, 0). Rather, there is a strong “elliptical” pattern centered at the (5.25, 0, 0) with additional scattering bulging out along the \mathbf{K} axis, which appears as shoulders in \mathbf{K} scan through (5.25, 0, 0). The intensity near (3.50, 0, 0) is from the tail of the strong \mathbf{q}_0 satellite at (3.25, 0, 0). In particular, the intensity asymmetry about the \mathbf{K} axis through (4, 0, 0) is due to the interference scattering (IFS) from the ortho-IV phase islands and the surrounding lattice-strain fields. Such interference effects have been known in the study of disorder and extensively discussed in Ref. 23.

The presence of HDS and IFS has to be taken into account in discussing the origin of the shoulders. The diffuse-scattering pattern around (4, 0, 0) shown in Fig. 2(a) suggests that the shoulders at (4.25, $\pm \delta$, 0) in Fig. 3(a) might be due to the lobes of HDS, extending roughly along [1 1 0] directions. But this scenario is unlikely to account for the strong shoulders of the (5.25, 0, 0) satellite given the absence of similar HDS around (5, 0, 0) Bragg peak.

The absence of HDS around (5, 0, 0) can be understood by examining the general nature of HDS.²³ As a long-range elastic distortion of the lattice, the strain fields give rise to HDS in the vicinity of a given Bragg point in proportion to the square of the unit-cell structure-factor modulus $|F(\mathbf{G})|^2 = |\sum_k f_k e^{-W_k(Q)} e^{i\mathbf{G}\cdot\mathbf{R}_k}|^2$, where \mathbf{G} is the Bragg point.²³ For YBCO_{6,92}, $|\frac{F(500)}{F(400)}|^2 \approx 0.02$. Using this ratio and the known intensity at (5.25, 0, 0) we estimate the HDS and IFS terms together to account for less than 5% of the intensity of (5.25, δ , 0) shoulders. Thus, the shoulders must be the fingerprint of a lattice modulation along the \mathbf{b} axis.

We first discuss the x-ray diffuse-scattering without considering the \mathbf{b} -direction modulation. With the presence of the ortho-IV phase islands and their surrounding strained lattice, the total diffuse-scattering intensity $I_{\text{diff}}(\mathbf{Q})$, can be written as in Eq. (1). A linear approximation is made assuming that the lattice distortions due to the strain are small. Here,

$$I_{\text{diff}}(\mathbf{Q}) \propto \left\langle \left| \sum_{j'l'k} f_k(Q) e^{-W_k(Q)} e^{-i\mathbf{Q}\cdot\mathbf{R}_{j'l'k}} (e^{-i\mathbf{Q}\cdot\mathbf{u}_{j'l'k}} - 1) + \sum_{lk} i\mathbf{Q}\cdot\mathbf{v}_{lk} f_k(Q) e^{-W_k(Q)} e^{-i\mathbf{Q}\cdot\mathbf{R}_{lk}} \right|^2 \right\rangle, \quad (1)$$

where j is the index for the $4a \times 1b \times 1c$ supercell²¹ in an ortho-IV minority phase island. $\mathbf{u}_{j'l'k}$ is the lattice distortion vector of the k th atom of the l' th unit cell inside the j th supercell. Outside of the island, $\mathbf{u}_{j'l'k}$ is zero and the first term vanishes. \mathbf{v}_{lk} is the lattice distortion of the k th atom of the l th unit cell due to the strain and the summation of the second term is over the whole crystal. $f_k(Q)$ and $e^{-W_k(Q)}$ are the atomic scattering factors and Debye-Waller factors, respectively. The modulus squared of the first term gives rise to the ortho-IV phase satellites, the modulus squared of the second term describes the HDS from lattice strain, and the interference of these two terms gives rise to IFS. The additional thermal diffuse scattering was calculated using the shell model by fitting to the measured phonon-dispersion curves²⁴ and subtracted from data except from those in Fig. 1. In our previous report,²¹ $\mathbf{u}_{j'l'k}$ has been fitted to the integrated intensities of a set of $\mathbf{G} \pm \mathbf{q}_0$ peaks (\mathbf{G} is a reciprocal-lattice vector) which were extracted by a careful line fitting procedure, and an ortho-IV displacement model was constructed without considering the \mathbf{q}_1 modulation.

Next, we need to incorporate the \mathbf{b} -direction modulation into Eq. (1). As discussed above, the \mathbf{b} -direction modulation does not form homogeneously throughout the whole crystal. Rather, a $\mathbf{q}_1 = (0, \delta, 0)$ -type wave vector acts as a \mathbf{b} -direction periodic modulation of the displacements of all the atoms involved in the ortho-IV phase.²¹ We incorporate this \mathbf{b} -direction modulation with a simple extension of the ortho-IV displacement pattern by replacing \mathbf{u} in Eq. (1) with \mathbf{t} as follows:

$$\mathbf{t}_{lk} = \mathbf{u}_{lk} [1 + d \cos(\mathbf{q}_1 \cdot \mathbf{R}_{lk})], \quad (2)$$

where l is the index of the unit cells inside the ortho-IV phase island and k is the atom index in that unit cell. Since the \mathbf{u}_{lk} , as reported in Ref. 21, lie in the \mathbf{a} - \mathbf{c} plane, the second term of Eq. (2) represents an additional transverse modulation along the \mathbf{b} direction. The second term contributes to the \mathbf{q}_1 shoulders and has small effects on \mathbf{q}_0 peaks. Thus fitted values of \mathbf{u}_{lk} remain close to those reported in Ref. 21 within the errors introduced by the IFS term included in this work.

To determine the values of δ and d , the experimental data are fitted with the ortho-IV model, together with the \mathbf{b} -direction lattice modulation as in Eq. (2). With this model the 2D pattern can be reproduced remarkably well as shown in Fig. 2(b). Figure 3 gives a better quantitative view of the data fit along important lines indicated in Fig. 2.

Thus, our experimental observation and quantitative analyses establish the existence of \mathbf{b} -direction lattice modulation with $\mathbf{q}_1=(0, \delta \approx 0.21, 0)$ within the ortho-IV phase islands in optimally doped YBCO.

III. DISCUSSION

The fact that \mathbf{q}_1 is very close to \mathbf{q}_{IC} strongly indicates that the observed \mathbf{b} -direction modulation within the ortho-IV phase islands is induced by the Fermi-surface (FS) effect. We emphasize that the model given in Eq. (2) corresponds to a modulation of the displacements of all the atoms within the ortho-IV phase islands (including those in the CuO_2 planes), rather than the atoms in the CuO chain plane along. In that sense, the observed \mathbf{b} -direction modulation does not correspond to the simple picture of a Kohn-Peierls $2k_F$ instability on a one-dimensional (1D) metallic chain. The short-range interchain correlation observed by STM (Refs. 14–16) also suggests that treating the CuO chains as pure 1D objects is over simplified. In our view, nested “ridges” (or “sheets”) of the FS induce a \mathbf{q}_1 amplitude modulation of the ortho-IV displacement pattern with a concomitant presence of a CDW on the CuO chains.

The idea that FS nesting can influence short-range order (SRO) and manifest itself in the x-ray diffuse scattering was discussed²⁵ in the study of order-disorder transitions in binary alloys such as Cu-Au and was used subsequently in investigations²⁶ of SRO correlated microdomain structures within a disordered matrix. In the context of the ortho-IV phase, any one of the four permutations of $\langle 1110 \rangle$ can form as antiphase (AP) domains with periodicity along the \mathbf{b} axis determined by \mathbf{q}_1 . These AP domains would also give shoulders to the \mathbf{q}_0 peaks in scans along the \mathbf{b}^* direction. However, structure-factor calculations based on various combinations (e.g., two $\langle 0111 \rangle$ and three $\langle 1110 \rangle$); as illustrated in Fig. 4) assuming no amplitude modulations of the ortho-IV displacement pattern²¹ did not yield relative intensities of \mathbf{q}_0 and \mathbf{q}_1 satellites consistent with the data. Although we cannot rule out a more subtle arrangement of AP domains, a simple transverse modulation of a monodomain ortho-IV pattern, as modeled in Eq. (2), adequately accounts for the data.

Our x-ray diffuse-scattering results are generally consistent with the STM observations^{14–16} which indicate that the CDWs are pinned by the oxygen vacancies in the CuO chains. Our finding that the \mathbf{q}_1 modulations are confined within ortho-IV islands seems to differ from STM reports^{14–16} of well-defined electronic corrugations existing in regions *away* from oxygen vacancies. This discrepancy may be due to energetics of CDW formation on chain-terminated surfaces as opposed to that in the bulk. The electronic structure calculations¹¹ indicate that the CuO chains in the bulk are on the verge of a CDW instability due to FS

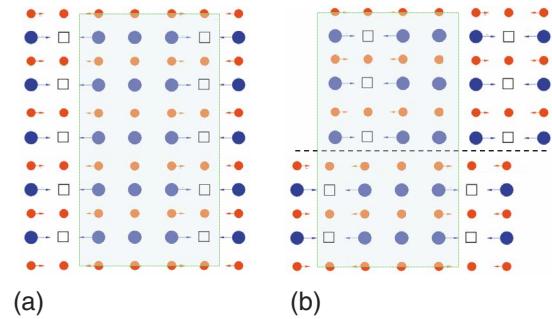


FIG. 4. (Color online) (a) Ortho-IV displacement pattern (ab plane) for the chains (Ref. 21). \mathbf{q}_1 further modulates amplitude of these displacements sinusoidally. (b) one possible AP domain with no modulations of displacement amplitudes. Small dots (red): Cu; big dots (blue): oxygen; squares: vacancy; dashed line: domain boundary; shaded area: 4×5 supercell.

nesting, but the formation of CDW depends on energy gains of carriers relative to the energy costs of the lattice distortions.²⁷ The lack of any peaks (or rods) near $(m, n, L) \pm \mathbf{q}_1$ suggests that the formation of CDW is suppressed by the rigidity of the average lattice. Rather, a static CDW can only be well established in favorable regions such as a cleaved surface with CuO chains on the first layer where the lattice is inevitably relaxed comparing with the bulk, or in elastically “softer” areas. Our previous x-ray studies²¹ have shown that ortho-IV islands are softer than the average lattice, which in principle favors the CDW formation. This agrees well with the STM observations^{14–16} of enhanced CDW amplitudes in the vicinity of oxygen vacancies.

In conclusion, in optimally doped YBCO, a short-range lattice modulation induced by FS nesting associated with CuO-chain subsystem with wave vector $\mathbf{q}_1=(0, \sim 0.21, 0)$ is observed. The fact that the \mathbf{q}_1 modulation is confined within the ortho-IV phase islands dismisses the concern of coexistence of the CDW and superconductivity on the CuO chain subsystem as a general property of YBCO. Even though the \mathbf{q}_1 modulation is driven by the FS nesting of the CuO chains, the shoulders at $\mathbf{q}_0 \pm \mathbf{q}_1$ also get contributions from the atoms located in the BaO and CuO_2 planes in the ortho-IV islands rather than from the chains alone [Eq. (2)]. Thus the FS effects perturb the CuO_2 planes within the ortho-IV phase islands as well. How the \mathbf{b} -direction short-range modulation reported here affects the local and global superconductivities calls for further studies of FS effects in YBCO.

ACKNOWLEDGMENTS

Work at UCSD is supported by the Department of Energy (DOE) through Grant No. DE-FG02-03ER46084. Use of the APS is supported by the DOE Contract No. DE-AC02-06CH11357. Work at Houston is supported by the State of Texas through the Texas Center for Superconductivity at the University of Houston.

- ¹D. N. Basov, R. Liang, D. A. Bonn, W. N. Hardy, B. Dabrowski, M. Quijada, D. B. Tanner, J. P. Rice, D. M. Ginsberg, and T. Timusk, *Phys. Rev. Lett.* **74**, 598 (1995).
- ²R. Gagnon, S. Pu, B. Ellman, and L. Taillefer, *Phys. Rev. Lett.* **78**, 1976 (1997).
- ³J. R. Kirtley, C. C. Tsuei, A. Ariando, C. J. M. Verwijs, S. Harkema, and H. Hilgenkamp, *Nat. Phys.* **2**, 190 (2006).
- ⁴R. Harris, P. J. Turner, S. Kamal, A. R. Hosseini, P. Dosanjh, G. K. Mullins, J. S. Bobowski, C. P. Bidinosti, D. M. Broun, R. Liang, W. N. Hardy, and D. A. Bonn, *Phys. Rev. B* **74**, 104508 (2006).
- ⁵I. I. Mazin, A. A. Golubov, and A. D. Zaikin, *Phys. Rev. Lett.* **75**, 2574 (1995).
- ⁶D. K. Morr and A. V. Balatsky, *Phys. Rev. Lett.* **87**, 247002 (2001).
- ⁷R. Franco and A. A. Aligia, *Phys. Rev. B* **67**, 172507 (2003).
- ⁸A. Ghosh, *Phys. Rev. B* **73**, 012504 (2006).
- ⁹X. S. Ye and J. X. Li, *Phys. Rev. B* **76**, 174503 (2007).
- ¹⁰D. H. Lu, D. L. Feng, N. P. Armitage, K. M. Shen, A. Damascelli, C. Kim, F. Ronning, Z.-X. Shen, D. A. Bonn, R. Liang, W. N. Hardy, A. I. Rykov, and S. Tajima, *Phys. Rev. Lett.* **86**, 4370 (2001).
- ¹¹W. E. Pickett, H. Krakauer, R. E. Cohen, and D. J. Singh, *Science* **255**, 46 (1992).
- ¹²H. Haghghi, J. H. Kaiser, S. Rayner, R. N. West, J. Z. Liu, R. Shelton, R. H. Howell, F. Solal, and M. J. Fluss, *Phys. Rev. Lett.* **67**, 382 (1991).
- ¹³M. C. Schabel, C.-H. Park, A. Matsuura, Z.-X. Shen, D. A. Bonn, R. Liang, and W. N. Hardy, *Phys. Rev. B* **57**, 6107 (1998).
- ¹⁴H. L. Edwards, A. L. Barr, J. T. Markert, and A. L. de Lozanne, *Phys. Rev. Lett.* **73**, 1154 (1994).
- ¹⁵H. L. Edwards, D. J. Derro, A. L. Barr, J. T. Markert, and A. L. de Lozanne, *Phys. Rev. Lett.* **75**, 1387 (1995).
- ¹⁶M. Maki, T. Nishizaki, K. Shibata, and N. Kobayashi, *Phys. Rev. B* **72**, 024536 (2005).
- ¹⁷S. Krämer and M. Mehring, *Phys. Rev. Lett.* **83**, 396 (1999).
- ¹⁸B. Grévin, Y. Berthier, and G. Collin, *Phys. Rev. Lett.* **85**, 1310 (2000).
- ¹⁹Z. Yamani, B. W. Statt, W. A. MacFarlane, R. Liang, D. A. Bonn, and W. N. Hardy, *Phys. Rev. B* **73**, 212506 (2006).
- ²⁰H. A. Mook, P. Dai, K. Salama, D. Lee, F. Dögan, G. Aeppli, A. T. Boothroyd, and M. E. Mostoller, *Phys. Rev. Lett.* **77**, 370 (1996).
- ²¹Z. Islam, X. Liu, S. K. Sinha, J. C. Lang, S. C. Moss, D. Haskel, G. Srajer, P. Wochner, D. R. Lee, D. R. Haefner, and U. Welp, *Phys. Rev. Lett.* **93**, 157008 (2004).
- ²²D. de Fontaine, G. Ceder, and M. Asta, *Nature (London)* **343**, 544 (1990).
- ²³M. A. Krivoglaz, *X-Ray and Neutron Diffraction in Nonideal Crystals* (Springer, New York, 1996); P. H. Dederichs, *J. Phys. F: Met. Phys.* **3**, 471 (1973).
- ²⁴S. L. Chaplot, W. Reichardt, L. Pintschovius, and N. Pyka, *Phys. Rev. B* **52**, 7230 (1995).
- ²⁵S. C. Moss, *Phys. Rev. Lett.* **22**, 1108 (1969).
- ²⁶S. Hashimoto, *Acta Crystallogr., Sect. A: Cryst. Phys., Diffraction, Theor. Gen. Crystallogr.* **37**, 511 (1981).
- ²⁷C. Kittel, *Introduction to Solid State Physics*, 7th ed. (Wiley, New York, 1996).